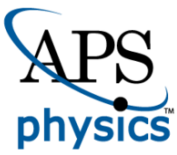

This is the accepted manuscript made available via CHORUS. The article has been published as:

Integral equation model for warm and hot dense mixtures

C. E. Starrett, D. Saumon, J. Daligault, and S. Hamel

Phys. Rev. E **90**, 033110 — Published 19 September 2014

DOI: 10.1103/PhysRevE.90.033110

An integral equation model for warm and hot dense mixtures

C. E. Starrett, D. Saumon and J. Daligault
Los Alamos National Laboratory, P.O. Box 1663, Los Alamos, NM 87545, U.S.A.

S. Hamel
Lawrence Livermore National Laboratory, Livermore, CA 94550, U.S.A
(Dated: September 3, 2014)

In Starrett and Saumon [Phys. Rev. E **87**, 013104 (2013)] a model for the calculation of electronic and ionic structures of warm and hot dense matter was described and validated. In that model the electronic structure of one 'atom' in a plasma is determined using a density functional theory based average-atom (AA) model, and the ionic structure is determined by coupling the AA model to integral equations governing the fluid structure. That model was for plasmas with one nuclear species only. Here we extend it to treat plasmas with many nuclear species, i.e. mixtures, and apply it to a carbon-hydrogen mixture relevant to inertial confinement fusion experiments. Comparison of the predicted electronic and ionic structures with orbital-free and Kohn-Sham molecular dynamics simulations reveals excellent agreement wherever chemical bonding is not significant.

PACS numbers: 52.27.-h, 52.27.Cm, 52.27.Gr

I. INTRODUCTION

Warm and hot dense matter refers to plasmas roughly as dense as solids up to thousands of times solid density. Temperatures range from approximately one eV up to several thousand eV. In nature such plasmas are found in a variety of astrophysical objects, including the cores of giant planets and in the envelopes of white dwarfs [1, 2]. Such plasmas are also of interest to the inertial confinement fusion community where these conditions are reached in implosion experiments [3]. Often the plasmas in question are mixtures. For example, $CH_{1.36}$[1] is of interest as an ablator material in inertial confinement fusion experiments at the National Ignition Facility (NIF) [4] and carbon/helium mixtures occur in white dwarf stars[1, 2].

One of the challenges of modeling warm and hot dense matter is to accurately calculate the electronic and ionic structures in a single model. Benchmark calculations have been made using density functional theory molecular dynamics (DFT-MD). This method is thought to be accurate and gives an essentially complete description of the plasma. Both Kohn-Sham (KS) [5, 6] and orbital-free (OF) [7] versions of DFT-MD exist. The primary limitation of these methods is their high computational cost. This is particularly acute for KS calculations, where a poor scaling of the computational cost with temperature limits it to low temperatures. The OF method does not suffer from this poor scaling but is still very expensive, typically limiting the number of particles in the MD simulation to a few 100's [8–11]. DFT-MD calculations are especially challenging for mixtures, where asymmetries in masses and number fractions increase the computational demands.

Starrett and Saumon presented an alternative method for calculating the electronic and ionic structures of warm and hot dense matter, in the form of pair distribution functions [12, 13]. Excellent agreement was found with corresponding DFT-MD simulations over a wide range of densities and temperatures. The principal advantage of this model is that it is much less computationally expensive than the corresponding DFT-MD simulations. The model uses a DFT based, average-atom (AA) approach to calculate the properties of one 'atom' in the plasma and couples this to the quantum Ornstein-Zernike (QOZ) equations for the ionic structure. The QOZ's are integral equations that can be rapidly solved, giving the ion-ion and ion-electron pair distribution functions. The AA model can be solved using either KS or OF functionals. A key assumption of the model is that the electronic density of the plasma can be written as a superposition of "pseudoatom" electron densities. The concept of the pseudoatom [14–16] is that of a charge neutral, atom-like entity with a nuclear charge at its origin, surrounded by a local, spherically symmetric electron cloud. This electron cloud comprises the electrons that are bound to the nucleus (together with the nucleus these form the ion), as well as screening electrons. The model of [12, 13] is, however, limited to homo-nuclear plasmas. Here we extend this model to hetero-nuclear plasmas, i.e. mixtures.

We first extend the QOZ equations to mixtures of quantal electrons and N types of classical ions. The result turns out to be a straightforward generalization of the corresponding N-component classical OZ equations, though the derivation is not trivial. Secondly, we show how the average-atom model developed in [12, 13] can be coupled to the QOZ's for mixtures. Lastly, we present an application of the model to $CH_{1.36}$ and compare the resulting electronic and ionic structures to OFMD and

[1] The notation means a carbon-hydrogen mixture in the ratio 0.424:0.576.

QMD[2] simulations.

The resulting complete model allows rapid calculation of the electronic and ionic structures of dense plasma mixtures (relative to DFT-MD) with no adjustable parameters. The extension to mixtures does not require any new physical approximations. Inputs to the model are the ion masses and nuclear charges, the number fractions of the ion species, as well as the plasma mass density and temperature. Lastly, we note that the model is all-electron, meaning that, unlike DFT-MD simulations, no pseudopotential is used when solving for the electronic structure.

The structure of this paper is as follows. In section II we develop the QOZ equations for arbitrary[3] multi-component fluids. We start by deriving the QOZ equations for a binary mixture (two classical ion species and quantal electrons). The extension to the N-component mixture is then obvious, and analogous to the corresponding classical OZ equations [17]. We then show how these equations can be written in terms of electronic screening densities of pseudoatoms, in analogy with the homo-nuclear case. The next step is to demonstrate how the QOZ equations can be mapped onto an effective N-component system, where the ions interact through short ranged, electron screened, effective potentials. Finally, we show how to calculate the screening densities for mixtures using the average-atom model developed in [12, 13]. In section VII we compare predictions of the electronic and ionic structures, in the form of pair distribution functions, to both quantum and orbital-free molecular dynamics simulations (QMD and OFMD). Finally, in section VIII we present our conclusions. Unless otherwise stated, atomic units, in which $\hbar = m_e = k_B = e = 1$, where the symbols have their usual meaning, are used throughout.

II. THE QUANTUM ORNSTEIN-ZERNIKE EQUATIONS FOR MIXTURES

We consider a mixture of N types of classical species with a neutralizing, responding, electron gas. The electrons and ions are in thermal equilibrium with temperature $T = 1/\beta$. The number fraction for ions of type i is x_i, such that

$$\sum_{i=1}^{N} x_i = 1. \tag{1}$$

If the charge of ion i is $\bar{Z}_i$, the average ionization of the plasma is

$$\bar{Z} = \frac{\bar{n}_e^0}{n_I^0} = \sum_{i=1}^{N} \bar{Z}_i x_i \tag{2}$$

where $\bar{n}_e^0$ is the average ionized electron particle density and n_I^0 is the average ion particle density. We also define the particle density for species i as

$$n_i^0 = x_i\, n_I^0 \tag{3}$$

A. The Quantum Ornstein-Zernike matrix

Chihara [18] derived the quantum Ornstein-Zernike (QOZ) equations for a mixture of one classical ion species and quantum mechanical electrons. Here we extend this derivation to a multi-component mixture of N-classical ions and quantum mechanical electrons. We start from the exact matrix equation [18] in k-space

$$\underline{\chi} = \left[\frac{\underline{C}}{\beta} + \left(\underline{\chi}^0\right)^{-1}\right]^{-1} \tag{4}$$

where the underline indicates a matrix. This formula relates the linear response functions $\underline{\chi}$ for an interacting system to those of a non-interacting system $\underline{\chi}^0$ and the direct correlation functions $\underline{C}$. For homogeneous system these are defined in real space as

$$\chi_{ij}(|\boldsymbol{r} - \boldsymbol{r}'|) = -\frac{\delta^2 \Omega}{\delta\Phi_i(\boldsymbol{r})\delta\Phi_j(\boldsymbol{r}')} \tag{5}$$

and

$$\frac{-1}{\beta} C_{ij}(|\,\boldsymbol{r} - \boldsymbol{r}'\,|) \equiv \left.\frac{\delta^2 \mathcal{F}^{ex}}{\delta n_i(\boldsymbol{r})\delta n_j(\boldsymbol{r}')}\right|_{V_i=0} \tag{6}$$

where

$$\Phi_i(\boldsymbol{r}) = \mu_i - V_i(\boldsymbol{r}) \tag{7}$$

is the intrinsic chemical potential for species i with particle density $n_i(\boldsymbol{r})$, chemical potential μ_i and external potential $V_i(\boldsymbol{r})$. Ω is the grand potential

$$\Omega = \mathcal{F} - \sum_{i}^{N+1} \int d\boldsymbol{r} \Phi_i(\boldsymbol{r}) n_i(\boldsymbol{r}), \tag{8}$$

$\mathcal{F}$ is the intrinsic free energy and

$$\mathcal{F} = \mathcal{F}^{id} + \mathcal{F}^{ex}. \tag{9}$$

$\mathcal{F}^{id}$ is the non-interacting intrinsic free energy and $\mathcal{F}^{ex}$ is the intrinsic free energy due to interactions [17]. The notation $V_i = 0$ indicates that the functional derivative is evaluated with the external potential set to zero. Finally,

[2] Quantum Molecular dynamics. This is DFT-MD with the orbital based Kohn-Sham method.

[3] Arbitrary meaning any number fraction and mass or charge ratio.

the matrices have size $(N+1)\times(N+1)$ for a system of electrons and N ion species and are symmetric.

To solve the matrix equation (4) we specialize to a mixture of quantal electrons (index e) and 2 classical ion species (indices 1 and 2). This greatly simplifies the problem and the solution to the general $(N+1)$ problem can be inferred from the result. We can use the fluctuation-dissipation theorem to relate the response functions χ to the corresponding structure factors S_{ij} [17] provided one of the particles (i or j) is classical,

$$\begin{aligned}\chi_{ij}(k) &= -\beta\sqrt{n_i^0 n_j^0}S_{ij}(k)\\ &= -\beta\sqrt{n_i^0 n_j^0}\left[\delta_{ij}+\sqrt{n_i^0 n_j^0}h_{ij}(k)\right] \qquad (10)\end{aligned}$$

where δ_{ij} is the Kronecker delta and $h_{ij}(k)$ is a pair correlation function. The (3×3) matrix in square brackets in equation (4) is now inverted, giving the QOZ equations for a binary mixture of classical ions and quantum electrons:

$$h_{ij}(k)=\left(-\frac{\chi^0_{jj}(k)}{\beta n_j^0}\right)\left[C_{ij}(k)+\sum_{\lambda=1}^{3}n_\lambda^0 h_{i\lambda}(k)C_{\lambda j}(k)\right] \qquad (11)$$

where the index $\lambda=3$ is for the electrons and the convention is that if either the i or j labels refer to an electron, then it is placed in the j position in equation (11) (recall the symmetry $h_{ij}=h_{ji}$).

By simple extension we can now write down the equations for the $(N+1)$ component plasma (N classical particles and quantum electrons)

$$h_{ij}(k)=\left(-\frac{\chi^0_{jj}(k)}{\beta n_j^0}\right)\left[C_{ij}(k)+\sum_{\lambda=1}^{N+1}n_\lambda^0 h_{i\lambda}(k)C_{\lambda j}(k)\right] \qquad (12)$$

where $\lambda=N+1$ is the index for the electrons. Equation (12) can be compared to the familiar expression for a mixture of $(N+1)$ classical particles [17] (see also equation (17)). The quantum nature of the electrons is embodied in the pre-factor $-\chi^0_{ee}(k)/(\beta\bar{n}_e^0)$. We note that χ^0_{ee} is the well-known finite temperature, non-interacting response function [19]. At zero temperature it is the Lindhard function [20]. For classical particles $\chi^0_{jj}(k)=-\beta n_j^0$ and the prefactor equals unity.

III. INTERPRETATION OF THE QOZ EQUATIONS AS A SYSTEM OF SCREENED IONS

The induced electronic screening density $n^{scr}_{i,e}(r)$ due to a weak external potential $-C_{ie}/\beta$ is given by linear response theory [21] as

$$n^{scr}_{i,e}(k)=-\frac{C_{ie}(k)}{\beta}\chi'_{ee}(k) \qquad (13)$$

where

$$\chi'_{ee}(k)\equiv\frac{\chi^0_{ee}(k)}{1+\chi^0_{ee}(k)C_{ee}(k)/\beta}. \qquad (14)$$

From equation (12) we therefore have

$$\Delta n_{i,e}(k)\equiv\bar{n}_e^0 h_{ie}(k)=n^{scr}_{i,e}(k)+\sum_{\lambda=1}^{N}n_\lambda^0 h_{i\lambda}(k)n^{scr}_{\lambda,e}(k) \qquad (15)$$

where

$$\Delta n_{i,e}(r) \;=\; n_{i,e}(r)-\bar{n}_e^0 \qquad (16)$$

and $n_{i,e}(r)$ is the spherically averaged electron density around an ion species i. The formula (15) says that for homogeneous plasmas and weak external potentials $C_{ie}(k)$, the electron density of the plasma is exactly written as the sum of spherically symmetric screening densities $n^{scr}_{i,e}(r)$. The QOZ equations can therefore be interpreted as relations for the structure of a fluid of classical ions whose interactions are screened by responding electrons with densities $n^{scr}_{i,e}(r)$.

IV. REDUCTION TO AN EFFECTIVE N-COMPONENT SYSTEM OF CLASSICAL PARTICLES

As in the homo-nuclear case, to solve the QOZ equations (12) for the ion-electron and ion-ion pair correlation functions h_{ie} and h_{ii} we make use of the interpretation given section III to map the QOZ equations onto their purely classical counterparts:

$$h_{IJ}(k) \;=\; C_{IJ}(k)+\sum_{\lambda=1}^{N}n_\lambda^0 h_{I\lambda}(k)C_{\lambda J}(k) \qquad (17)$$

This procedure has been extensively described for the homo-nuclear case [12, 22]; here we give only the salient details.

We assume that there exists an effective N-component system of classical particles, interacting through short ranged pair potentials $V_{IJ}(r)$ such that the ion-ion pair correlation functions h_{IJ} are identical to those of a corresponding[4] $(N+1)$-component system of classical particles and quantal electrons. The ion-ion closure relation for the effective N-component system is

$$h_{IJ}(r)+1=\exp\left(-\beta V_{IJ}(r)+h_{IJ}(r)-C_{IJ}(r)+B_{IJ}(r)\right) \qquad (18)$$

where $I,J=1,\ldots,N$ and the $B_{IJ}(r)$ are the bridge functions [17]. Similarly, for the $(N+1)$ component system we have

$$h_{ij}(r)+1=\exp\left(-\beta\frac{\bar{Z}_i\,\bar{Z}_j}{r}+h_{ij}(r)-C_{ij}(r)+B_{ij}(r)\right) \qquad (19)$$

[4] Corresponding meaning that the classical particles have the same charge, mass and number densities.

where $i, j = 1, \ldots, N$ and $\bar{Z}_i$ is the charge of ion i. By assuming that $h_{ij} = h_{IJ}$ and $B_{ij} = B_{IJ}$, one uses the QOZ and OZ equations (12) and (17) with equations (18) and (19) to relate the pair potentials to the screening densities:

$$V_{IJ}(k) \;=\; \frac{4\pi \bar{Z}_i \bar{Z}_j}{k^2} - \frac{C_{ie}(k)}{\beta} n_{j,e}^{scr}(k). \qquad (20)$$

Recall that the ion-electron direct correlation functions $C_{ie}(k)$ are also related to the screening densities via equation (13).

The problem of solving the QOZ equations (12) is now reduced to solving their purely classical counterparts (equations (17)) for given pair potentials V_{IJ}, using the ion-ion closure relations (18). To determine the potentials (20) we need the screening densities $n_{i,e}^{scr}(k)$ for each ion and the electron-electron direct correlation function $C_{ee}(k)$ (equation (14)). For the latter we use the jellium approximation which was successful for the homo-nuclear case [13]. To determine the screening densities we also use the same approximation as for the homo-nuclear case, i.e. we determine them using an average-atom model.

V. THE AVERAGE-ATOM MODEL FOR THE SCREENING DENSITY

For the homo-nuclear case the method for calculating the screening density is described in detail in [12, 13]. It is summarized here to provide a basis for its extension to mixtures. We assume that the electron density of the plasma is given by a superposition of charge neutral 'pseudoatom' electron densities. Conceptually, the pseudoatom electron density $n_e^{PA}(r)$ is a local, spherically symmetric electron cloud that contains both the bound states, with electron density $n_e^{ion}(r)$, and the screening electrons ($n_e^{scr}(r)$) that contribute to the valence electrons

$$n_e^{PA}(r) = n_e^{ion}(r) + n_e^{scr}(r). \qquad (21)$$

Clearly, the superposition approximation will be excellent for deeply bound states, and equation (15) demonstrates that it is also appropriate for the valence states provided these states can be reasonably well represented by linear response theory. It becomes inaccurate in thermodynamic regimes where a significant fraction of the atoms in the plasma form molecules.

To calculate $n_e^{PA}(r)$ we consider a system with a nucleus at the origin, surrounded by a spherically averaged ion distribution (the 'full' system). The electron density $n_e^{full}(r)$ for this system is found by minimizing the free energy for a given kinetic energy functional (eg. Kohn-Sham or Thomas-Fermi) and a given exchange-correlation functional. We then consider a system with the same spherically averaged ion distribution but no central nucleus (the 'external' system). The electron density $n_e^{ext}(r)$ for this external system is found in the same way as for the full system. The difference in these electron densities defines the pseudoatom electron density

$$n_e^{PA}(r) = n_e^{full}(r) - n_e^{ext}(r). \qquad (22)$$

The screening density is then obtained after defining the electron density of bound states (equation (21))

The above procedure requires a knowledge of the spherically averaged ion distribution. This distribution is given by the ion-ion pair distribution function $g(r)(= h(r) + 1)$. In the ion-sphere (IS) version of the homo-nuclear model [13], we solve for the screening density, as we have described above, with $g(r)$ set to be a step function at the ion-sphere radius R

$$g(r) = \Theta(r - R) \qquad (23)$$

where

$$\frac{4\pi R^3}{3} = V^{ion} = \frac{M}{\rho} \qquad (24)$$

and V^{ion} is the volume per ion, which is determined from input of the mass density ρ and atomic mass M. In [13] it was shown that the $g(r)$ from this IS model is very close to that of a self-consistent version of the model, where the calculated $g(r)$ is fed back as input to the AA model, and the cycle repeated until converged. This result was explained in [13] by noting that in the linear response regime $n_e^{scr}(r)$ is fully independent of $g(r)$.

The same technique for determining the screening densities can be applied here for mixtures, where now an AA model is solved for each component. Because of the demonstrated insensitivity of $n_e^{scr}(r)$ to $g(r)$ we use the ion-sphere (IS) AA model [13], both in the QM and TF versions of the model (referred to as IS-QM and IS-TF). For species i the ion-sphere radius R_i is related the volume per ion V_i^{ion} but, unlike the homo-nuclear case, the volumes V_i^{ion} are not uniquely determined from input. The volumes do however, satisfy

$$\sum_{i=1}^{N} x_i V_i^{ion} \;=\; \frac{\sum_{i=1}^{N} x_i \, M_i}{\rho}. \qquad (25)$$

where M_i is the atomic mass of species i. Further, the chemical potentials μ_e^i of the electrons for each average atom ($i = 1, \ldots, N$) must be equal

$$\mu_e^i = \mu_e \qquad (26)$$

The solution of the AA provides a relation between μ_e^i and V_i^{ion}. Thus, the set of V_i^{ion} are adjusted to satisfy equations (25) and (26), with μ_e a priori unknown. The solution can be sped up considerably by pre-tabulating μ_e^i as a function of V_i^{ion} and T for the species of interest. Thus we obtain a single electron chemical potential for the mixture, bound and continuum wave functions and the nucleus-electron interaction potentials as well as the ion and screening densities for each ion species.

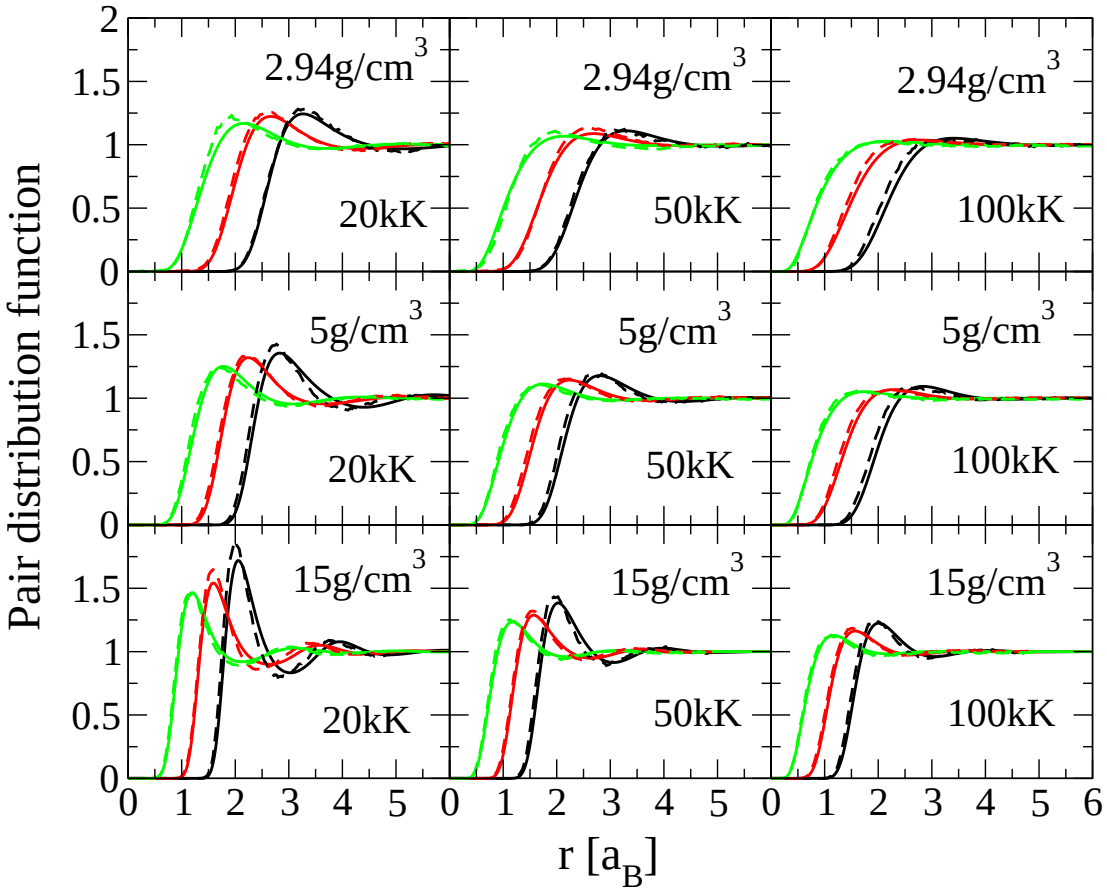

FIG. 1: (color online) Ion-ion pair distribution functions for $CH_{1.36}$. IS-TF (solid lines) compared to OFMD simulation results (dashed lines) in the TF approximation. C-C in black (right-most lines), C-H in red (middle lines) and H-H in green (left-most lines).

VI. PAIR DISTRIBUTION FUNCTIONS

The above model allows us to determine the ion-ion and electron-ion pair distribution functions, $g_{ij}(r)$ and $g_{ie}(r)$ respectively. $g_{ij}(r)$ is simply related the pair correlation functions $h_{ij}(r)$

$$g_{ij}(r) = 1 + h_{ij}(r) \tag{27}$$

The all-electron, electron-ion pair distribution functions are given by

$$g_{ie}(r) = \frac{n_{i,e}^{all}(r)}{n_e^{all}} \tag{28}$$

where

$$n_e^{all} = \sum_{\lambda=1}^{N} n_\lambda^0 Z_\lambda \tag{29}$$

is the average electron density of all electrons in the plasma (including bound electrons), Z_λ is the nuclear charge of species λ, and the spherically averaged electron density about a nucleus of species i is

$$n_{i,e}^{all}(r) \equiv n_{i,e}^{PA}(r) + \sum_{\lambda=1}^{N} n_\lambda^0 \int d^3r' g_{i\lambda}(|\boldsymbol{r} - \boldsymbol{r}'|) n_{\lambda,e}^{PA}(\boldsymbol{r}') \tag{30}$$

This last equation is a generalization of equation (15) to all-electrons and written in real space.

VII. COMPARISON WITH DFT-MD SIMULATIONS

All calculations with the new model have been carried out using the Dirac exchange functional [23] and the HNC closure relation in which $B_{II} = B_{IJ} = B_{JJ} = 0$. The latter approximation is not necessary since bridge function approximations exist [24–27], but is adequate for the present purposes. The bridge function will become important for strong coupling cases.

In figure 1 we compare ion-ion pair distribution functions $g_{ij}(r)$ from the new model in the TF approximation

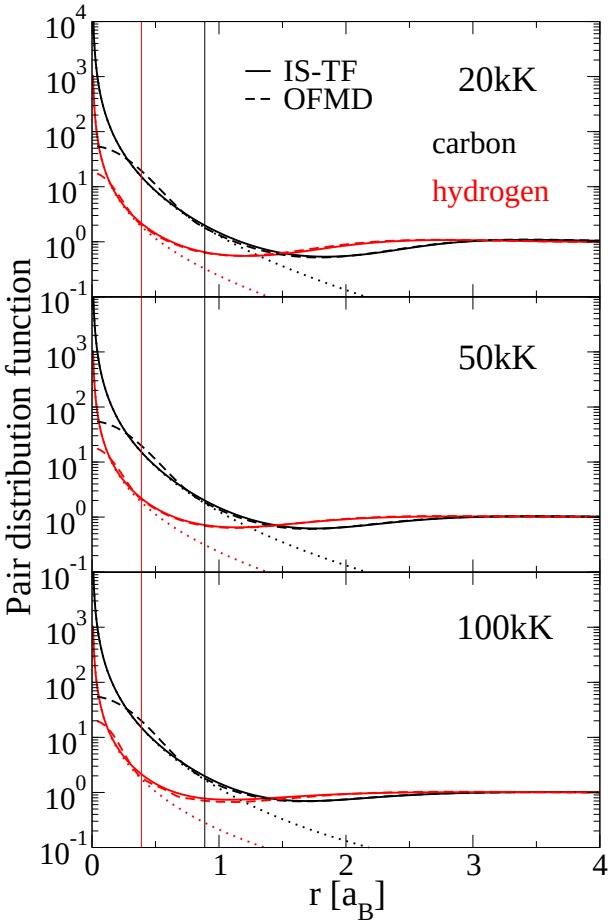

FIG. 2: (color online) IS-TF ion-electron pair distribution functions for $CH_{1.36}$ at 2.94g/cm^3, compared to OFMD simulation results in the TF approximation. Carbon in black (right-most lines), hydrogen in red (left-most lines). Solid lines are IS-TF, dashed lines are OFMD. Also shown (dotted lines) is the contribution to $g_{ie}(r)$ from $n_e^{PA}(r)$ alone. The thin vertical lines indicate the cutoff radius r_c used to generate the pseudopotentials for H (left) and C (right) in the OFMD simulations.

(IS-TF) to OFMD simulations for $CH_{1.36}$, which is close to the stochiometry of the plastic ablator used in inertial confinement capsules [3, 4]. The OFMD simulations use the same exchange potential [23] and the TF functional, and so are directly comparable to the IS-TF calculations, and were carried out using 250 particles (106 Carbon + 144 Hydrogen) in a cubic cell with periodic boundary conditions. The Hartree potential is calculated with FFT on a regular grid with 64^3 grid points and the time step is $0.01\omega_p$, where ω_p is the plasma frequency. The agreement between IS-TF and OFMD is very good to excellent for all densities and temperatures, for all three pair distribution functions (C-C, C-H and H-H). The largest difference is seen for the highest density and lowest temperature, where the ion-ion coupling is the strongest. The differences seen in this regime likely stem from the use of the HNC ion-ion closure relation, which becomes less accurate when the coupling is strong.

In figure 2 ion-electron pair distribution functions $g_{ie}(r)$ corresponding to the lowest density calculations in figure 1 are shown. Again, the agreement between the IS-TF model and the OFMD simulations is excellent for all three temperatures. The OFMD simulations use a pseudopotential which removes the Coulombic divergence in the electron-ion interaction potential and replaces it with a well behaved, but artificial, pseudo-potential [28]. For this reason we do not expect the OFMD electron densities to be accurate for $r < r_c$, where the actual potential has been replaced by the pseudopotential. The OFMD simulations return a finite value for $g_{ie}(r)$ at $r = 0$, in contrast to the IS-TF results which exhibit the correct divergent behavior ($\lim_{r\to 0} g_{ie}(r) \to r^{-3/2}$). This highlights an advantage of the IS-TF method over OFMD, i.e. it is an all-electron model so no pseudopotential is needed.

Next we turn to comparison between IS-QM and DFT-MD where both use the Kohn-Sham functional for the same cases of a $CH_{1.36}$ mixture. Our QMD simulations are performed using the Vienna ab initio Simulation Package (VASP) [29]. Born-Oppenheimer MD within the NVT-ensemble with a Nosé-Hoover thermostat [30, 31] is used throughout. We use a time step of 0.2 fs except for the very highest temperatures of our study, where we need to use a 0.1 fs time step in order to converge the internal energy and pressure to the desired accuracy. We use the generalized gradient approximation (GGA) of DFT with the Perdew-Burke-Ernzerhof (PBE) [32, 33] exchange-correlation functional. Projector-augmented wave (PAW) [34, 35] pseudopotentials are used to account for the core electrons. We used the harder potentials for C and H in the VASP PAW library (with core radii of 1.1 and 0.8 a.u. respectively). The plane-wave cutoff is set to 1300 eV. The electronic density is constructed from single-particle wave functions by sampling only at the $(\frac{1}{4}, \frac{1}{4}, \frac{1}{4})$ of the Brillouin zone. The $CH_{1.36}$ mixture was simulated with 236 atoms (100 C and 136 H) We also conducted pure carbon simulations (see below) with 64 atoms.

The comparison of ion-ion pair distribution functions is shown in figure 3. The agreement is very good for higher temperatures and higher densities, but degrades considerably at the lower temperatures and densities. To elucidate the origin of this disagreement we compare in figure 4 ion-ion pair distributions for pure carbon (i.e. not a mixture), over a similar range of conditions. A similar trend in agreement with respect to density and temperature is seen. This indicates that it is not the extension of our model to mixtures that is the source of the disagreement, but rather that the approximations involved in IS-QM are breaking down at the lowest temperatures and densities for carbon. Angular distribution functions extracted from the simulations of pure carbon (not shown) indicate angular preference in nearest neighbor positions for the lower temperatures and densities

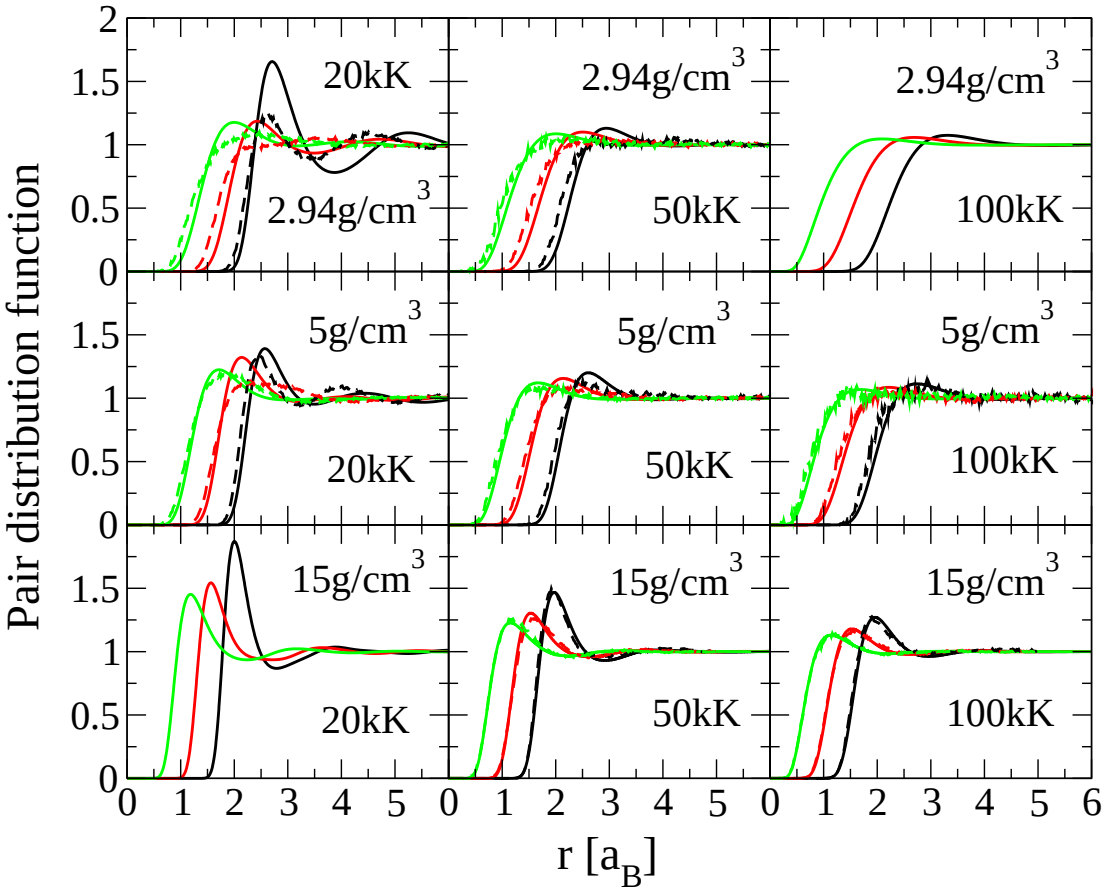

FIG. 3: (color online) Ion-ion pair distribution functions for $CH_{1.36}$. IS-QM (solid lines) compared to QMD simulations (dashed lines). C-C in black (right-most lines), C-H in red (middle lines) and H-H in green (left-most lines). For panels with only IS-QM curves, corresponding QMD results were not available.

in figure 4. This implies that significant bonding between the carbon atoms remains at these temperatures and densities. Such bonding is not captured in the IS-QM model which approximates the electron density as a superposition of spherically symmetric pseudoatoms. In contrast to this disagreement, in [12] good agreement with QMD simulations for aluminum was found at solid density ($2.7 g/cm^3$) and down to 2eV (23.2kK). Clearly the fact that aluminum forms a simple liquid favors the superposition approximation. While for carbon and $CH_{1.36}$, strong bonding and angular effects must be overcome by increasing the density or temperature before the model becomes accurate. This is supported by the fact that there is good agreement with OFMD simulations for $CH_{1.36}$, for the same conditions, where the use of the TF functional in the OFMD simulations precludes bonding effects (though not other angular effects). The excellent agreement between IS-QM and QMD for $CH_{1.36}$ at $15 g/cm^3$ at 100kK is expected to continue to higher densities and temperatures. For higher temperatures than shown QMD quickly becomes prohibitively expensive, whereas IS-QM remains tractable up to thousands of eV.

VIII. CONCLUSIONS

A model for the rapid calculation of the electronic and ionic structures of warm and hot dense mixtures has been presented. This is an extension of a previous model [12, 13] for homo-nuclear plasmas. Comparisons with DFT-MD simulations for $CH_{1.36}$ demonstrate excellent agreement on the ionic and electronic structures for Thomas-Fermi based calculations, while agreement between Kohn-Sham based calculations is excellent for higher temperatures and densities but becomes poor at lower temperatures and densities. A similar result is found by comparing Kohn-Sham based calculations for a pure carbon plasma under similar conditions. Such disagreement had not been previously observed in comparisons for a pure aluminum plasma [12]. This is explained as a breakdown of the superposition approximation which underpins the model, as it cannot describe the bonding between carbon atoms observed in the Kohn-Sham DFT-

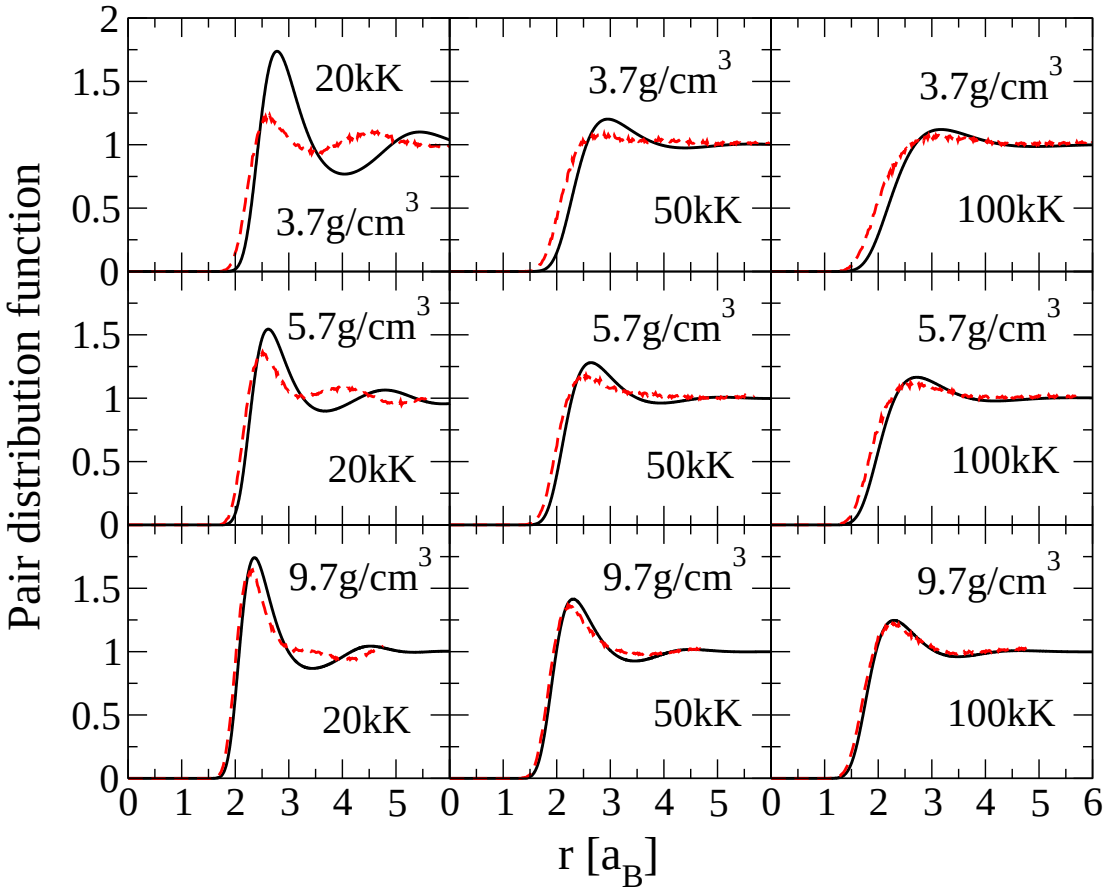

FIG. 4: (color online) Ion-ion pair distribution functions for pure C. IS-QM (solid lines) compared to QMD simulations (dashed lines).

MD simulations.

These initial comparisons indicate that the method is a promising technique for calculating electronic and ionic structures where bonding is not significant. In addition the method is very rapid relative to the corresponding DFT-MD simulations. Thomas-Fermi based calculations with the new model take a few minutes on an single processor while Kohn-Sham based calculations can take a few hours[5]. Moreover, the model is all electron, meaning that no pseudopotential is used, in contrast to DFT-MD simulations. We note that the Kohn-Sham version of the model can access the high temperature regime (1000's of eV), something that is not computationally tractable with Kohn-Sham DFT-MD. Another advantage of the model is that highly asymmetric mixtures (i.e. high mass ratios, charge ratios or extreme mixing fractions) present no additional difficulties, in contrast with DFT-MD simulations. Finally we note that the model could be used as the basis for predicting X-ray scattering spectra [36] and for calculating ionic transport properties on the basis of effective potential theory [37].

[5] Our IS-QM calculations use a shared memory, OpenMP parallel routine to solve for the continuum states [13].

Acknowledgments

This work was performed under the auspices of the United States Department of Energy under contract DE-AC52-06NA25396 and LD-RD grant number 20130244ER.

[1] Report of ReNew workshop. *Basic research needs for high energy density laboratory physics.* U.S. Department of Energy, 2009. http://science.energy.gov/~/media/fes/pdf/workshop-reports/Hedlp_brn_workshop_report_oct_2010.pdf.

[2] G. Chabrier and E. Schatzmann. *IAU Colloquium 147,*

The Equation of State in Astrophysics. Cambridge, 1994.
[3] B. A. Hammel, S. W. Haan, D. S. Clark, M. J. Edwards, S. H. Langer, M. M. Marinak, and M. V. Patel. *High energy density physics*, 6:171, 2010.
[4] Sebastien Hamel, Lorin X. Benedict, Peter M. Celliers, M. A. Barrios, T. R. Boehly, G. W. Collins, Tilo Döppner, J. H. Eggert, D. R. Farley, D. G. Hicks, J. L. Kline, A. Lazicki, S. LePape, A. J. Mackinnon, J. D. Moody, H. F. Robey, Eric Schwegler, and Philip A. Sterne. *Phys. Rev. B*, 86:094113, 2012.
[5] S. Mazevet, M. P. Desjarlais, L. A. Collins, J. D. Kress, and N. H. Magee. *Phys. Rev. E*, 71:016409, 2005.
[6] M. P. Desjarlais, J. D. Kress, and L. A. Collins. *Phys. Rev. E*, 66:025401(R), 2002.
[7] G. Zérah, J. Clérouin, and E. L. Pollock. *Phys. Rev. Lett.*, 69:446, 1992.
[8] J.-F. Danel, L. Kazandjian, and G. Zérah. *Phys. Plasmas.*, 13:092701, 2006.
[9] J.-F. Danel, L. Kazandjian, and G. Zérah. *Phys. Plasmas.*, 15:072704, 2008.
[10] J.-F. Danel, L. Kazandjian, and G. Zérah. *Phys. Plasmas.*, 19:122712, 2012.
[11] P. Arnault, J. Clérouin, G. Robert, C. Ticknor, J. D. Kress, and L. A. Collins. *Phys. Rev. E*, 88:063106, 2013.
[12] C. E. Starrett and D. Saumon. *Phys. Rev. E*, 87:013104, 2013.
[13] C. E. Starrett and D. Saumon. *High Energy Dens. Phys.*, 10:35, 2014.
[14] F. Perrot. *Phys. Rev. A*, 42:4871, 1990.
[15] L. Dagens. *J. Phys. C*, 5:2333, 1972.
[16] J. M. Ziman. *Proc. Phys. Soc.*, 91:701, 1967.
[17] J-P. Hansen and I.R. McDonald. *Theory of simple liquids, Third edition*. Academic press, 2006.
[18] J. Chihara. *J. Phys. C: Solid State Phys.*, 17:1633, 1984.
[19] G. Chabrier. *J. Phys. France*, 51:1607, 1990.
[20] S. Ichimaru. *Statistical plasma physics, Volume II: Condensed plasmas*. Westview Press, 2004.
[21] N. W. Ashcroft and D. Stroud. *Sol. State Phys.*, 33:1, 1978.
[22] J. A. Anta and A. A. Louis. *Phys. Rev. B*, 61:11400, 2000.
[23] P. A. M. Dirac. *Proc. Cambridge Philos. Soc.*, 26:376, 1930.
[24] G. Faussurier. *Phys. Rev. E*, 69:066402, 2004.
[25] Y. Rosenfeld. *J. Stat. Phys.*, 42:437, 1986.
[26] H. Iyetomi, S. Ogata, and S. Ichimaru. *Phys. Rev. A*, 46:1051, 1992.
[27] W. Daughton, M. S. Murillo, and L. Thode. *Phys. Rev. E*, 61:2129, 2000.
[28] F. Lambert, J. Clérouin, and G. Zérah. *Phys. Rev. E*, 73:016403, 2006.
[29] G. Kresse and J. Furthmüller. *Phys. Rev. B*, 54:11169, 1996.
[30] S. Nosé. *Chem. J. Phys.*, 81:511, 1984.
[31] W. G. Hoover. *Phys. Rev. A*, 31:1695, 1985.
[32] J. P. Perdew, K. Burke, and M. Ernzerhof. *Phys. Rev. Lett*, 77:3865, 1996.
[33] J. P. Perdew, K. Burke, and M. Ernzerhof. *Phys. Rev. Lett*, 78:1396, 1997.
[34] P. E. Blochl. *Phys. Rev. B*, 50:17953, 1994.
[35] G. Kresse and D. Joubert. *Phys. Rev. B*, 59:1758, 1999.
[36] A. N. Souza, D. J. Perkins, C. E. Starrett, D. Saumon, and S. B. Hansen. *Phys. Rev. E*, 89:023108, 2014.
[37] Scott D. Baalrud and Jérôme Daligault. *Phys. Rev. Lett.*, 110:235001, 2013.